An Atomistic Perspective on Twinning Phenomena in Nano-enhanced fcc Metals

Frederic Sansoz, Hanchen Huang, and Derek H. Warner

Twin boundaries exist in bulk metals, and they are even more common in metallic nanomaterials. Molecular simulation has made it possible to achieve a predictive understanding of the atomic mechanisms leading to the enhanced properties of nano-twinned metals. Taking nanowires as prototypes, this paper presents an atomistic view of twin structure and its important role in synthesis and in mechanical deformation.

INTRODUCTION

Twin boundaries are present in various crystalline structures. This paper focuses on face-centered-cubic (fcc) metals. Twin boundaries are special interfaces in fcc metals. As a homointerface–grain boundary interface, a twin boundary has very low formation energy and formation volume.[1] An atom at the twin boundary has exactly the same coordination (number of first nearest neighbors) as its bulk counterpart; in contrast, an atom at random boundaries generally has very different coordinations. On the other hand, twin boundaries are often seen as having no interfaces, since the local structure near a twin boundary is perfect hexagonal-close-packed (hcp). Therefore, the twin formation energy is related to the energy difference between fcc and hcp structures.

Taking copper as an example, the binding energy difference of hcp and fcc is 0.01 eV/atom, and the corresponding twin formation energy is 0.0014 eV/A^2.[2] Like the formation energy, atomic structure near a twin boundary also reflects the interplay of fcc and hcp structures. The fcc {111} and hcp {0001} planes are the most closed packed and have the same hexagonal arrangements of atoms. In fcc, three {111} planes form one period in the form of ABCABCABC stacking; in hcp, two {0001} planes form one period in the form of ABABABAB stacking. Near a twin boundary, the stacking order becomes ABCA**B**ACBA; where the highlighted **B** plane is the twin boundary.

The twin boundary formation can become substantially easier near surfaces, which are abundant in nanowires. When an adatom is deposited on the Cu{111} surface, it may occupy either an fcc or an hcp lattice site and the energy difference is only 0.01 eV.[3] In addition to the lower energy required to nucleate a twin near surfaces, surface reconstruction/stress is another factor affecting twin formation in nanometals. Twinning facilitates the reconstruction and release surface stress, leading to "multiply twinned particles."[4] Since the twins are ubiquitous in nanometals, they must be designed and controlled in synthesis and application. This paper reviews the manipulation of twins in synthesis, and understanding of their effects in mechanical deformation of nano-engineered metals, including nano-wires, -rods, and -pillars, and nano-twinned metal thin films.

How would you…

…describe the overall significance of this paper?

This paper provides atomistic insight into the fundamental mechanisms governing the enhanced properties of face-centered cubic metallic nanomaterials with twin boundaries. The importance of nanoscale twins in the synthesis of nanowires, and their mechanical properties including dislocation-twin boundary interactions and twin nucleation, is addressed.

…describe this work to a materials science and engineering professional with no experience in your technical specialty?

The importance of twin boundaries, a special type of interface in crystalline materials, is ubiquitous during both synthesis and mechanical deformation of nanoscale fcc metals. This paper describes how atomistic modeling and simulation can provide a predictive understanding of twinning phenomena in the synthesis of fcc metal nanowires, their strength, and plastic deformation.

…describe this work to a layperson?

A twin boundary is a special type of planar defect which can be used to enhance the properties of crystalline materials at atomic scale. This paper demonstrates how computer simulation can help to study the fundamental mechanisms leading to the enhanced properties of metals containing nanometer-scale twin boundaries. Such an approach can help engineers achieve a predictive understanding of the structure-properties relationship in these materials.

SYNTHESIS OF NANOWIRES

Twins naturally form during nanowire synthesis.[5] Since the energetic preference for an adatom on an fcc site (over an hcp site) is small, twin nucleation is readily realizable. This alone would have not guaranteed large populations of twin boundaries, since growth of twin boundaries may encounter higher energy barriers. However, additional energy is gained in forming twin boundaries in nanowires. Without the twin boundary, it is impossible to cover the sides of a <111> nanowire with all or predominantly {111} surfaces, which are energetically favorable. The twin formation makes this coverage possible, as schematically illustrated

in Figure 1a. Both molecular dynamics simulations[6] and magnetron sputtering deposition[7] have confirmed such twin formations and {111} coverage. Note that the surface energy minimization also drives twin formation in other cubic nanowires, such as SiC nanowires;[8,9] the Wulff construction of SiC contains {111} surfaces only. The presence of twin boundaries in nanowires leads to interesting mechanical characteristics, as discussed in the next section.

Beyond the natural occurrence in nanowires, twin boundaries can be manipulated to realize directed assembly of hierarchical nanostructures. In an fcc crystal, there are four {111} planes, and a twin boundary can form on any of the four. When two twin boundaries from two different {111} planes meet, their intersection is a Σ9 grain boundary,[10] shown as "I" in Figure 1b. The Σ9 grain boundary is energetically similar to random grain boundaries, and its high energy drives atoms away from it and triggers the bifurcation of nanowire. This property of twin boundaries, when coupled with geometrical shadowing and kinetics-limited length scale, enables the self-assembly of the Y-shaped nanowire of Figure 1b. The geometrical shadowing effect enhances axial growth while minimizing lateral expansion. The kinetics defines characteristic length scales during surface processing. Specifically, the newly identified three-dimensional Ehrlich–Schwoebel barrier[11,12] defines a new characteristic length scale—the dimension of surface islands bounded by multiple-layer steps.[13] Because of this length scale, the bifurcated nanowire of Figure 1b continues to grow axially without too much lateral expansion. Both molecular dynamics simulations and magnetron sputtering deposition have also confirmed this conceptualized self-assembly of Y-shaped nanowire.[10]

DISLOCATION–TWIN BOUNDARY INTERACTIONS

Strengthening Effects in Twinned Nanowires and Bulk Metals

Nanoscale growth twins are known to strongly influence the plastic behavior of bulk metals with low stacking energy such as pure copper and austenitic stainless steels, as reviewed elsewhere in this issue.[14] In bulk nanotwinned metals, a decrease of twin interspacing (i.e., the average distance that a dislocation needs to span when traveling from one twin boundary to another during plastic deformation) results in a dramatic increase in material strength and hardening at the nanoscale. The transmission of edge and screw dislocations across coherent Σ3 twin boundaries has been simulated in fcc metals using atomistic methods to understand the role of dislocation–twin boundary interactions on mechanical behavior.[15–25] It was shown that screw dislocations, which have a Burgers vector parallel to the twin plane, can either propagate into the adjacent twin grain by cutting through the boundary or be absorbed and dissociate within the boundary plane by cross-slip, depending on the stacking fault energy of the metal.[19,21] In addition, the resistance to slip propagation across twin interfaces that may result in strengthening effects strongly depends on the nature of interfacial plasticity and underlying dislocation pathways at the boundaries.[23,24]

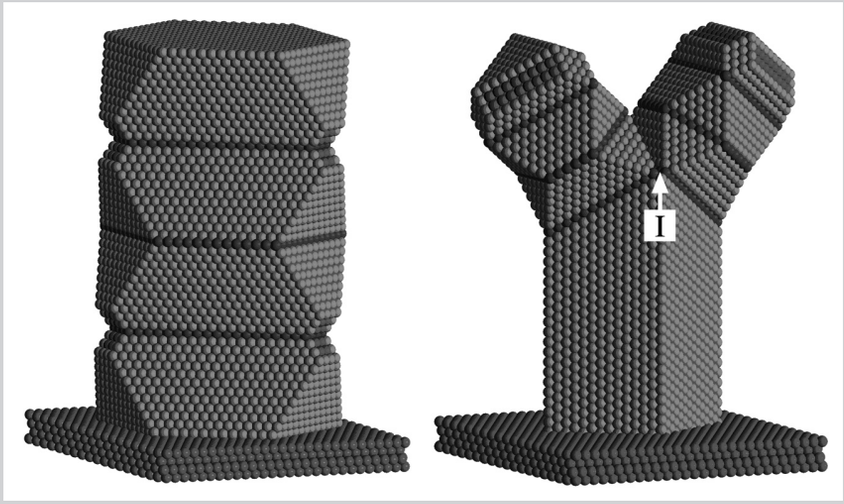

a b

Figure 1. (a) A schematic of <111> nanowire with sides being predominantly {111} plus {100}; (b) a schematic of Y-shaped nanowire formation through twin boundary intersection.

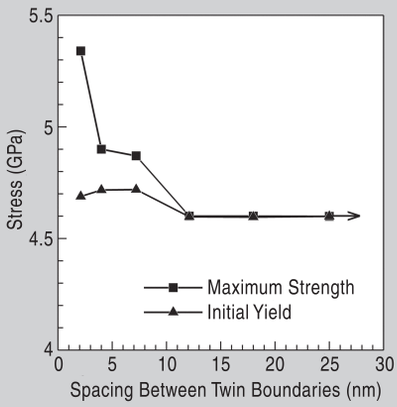

Figure 2. Strengthening effects in <111>-oriented gold nanopillars under compression due to pre-existing coherent Σ3 twin boundaries. Simulated yield stress and maximum strength as a function of mean spacing between twin boundaries are shown. The yield point is defined by the nucleation of the very first lattice dislocation during deformation. The nanopillar was 12 nm in diameter and 36 nm in height in all the simulations.

Similarly, all experimental evidence shows that fcc metal nanowires can be significantly hardened by pre-existing coherent Σ3 twin boundaries.[26,27] A first attempt to characterize the effect of one growth twin boundary located inside a <111>-oriented gold nanowire has been made by B. Hyde et al.[18] using atomistic simulation. These authors concluded that the twin itself was an effective obstacle against the propagation of dislocations. In twinned copper nanowires, J. Wang and H. Huang[20] also discovered that the nature of the slip changes when partial dislocations are transmitted across a twin boundary (i.e., upon penetration) a dislocation with Burgers vector of ½<110> can nucleate and glide on a {100} plane instead of conventional {111} planes.

The role of several growth twin boundaries on the slip activity and strengthening of metallic nanowires and nanopillars has also been investigated in gold[22] and copper[28,29] using molecular dynamics simulation. In <111>-oriented gold nanopillars containing several coherent Σ3 twin boundaries, K.A. Afanasyev and F. Sansoz[22] have predicted that a reduction in twin interspacing causes a significant increase in maximum strength without a notable change in yield stress when the very first lattice dislocation is nucleated (Figure 2). This observation therefore supports the hypothesis that the interaction between lattice dislocations and twin boundaries could be a dominant factor in the strengthening process of twinned fcc metal nanowires.

Mechanistic Interactions between Dislocation and Twin Boundary

To better interpret the mechanical strengthening effects induced by preexisting twins in fcc metal nanowires, Figure 3 presents the details of the dislocation dynamics at the intersection between a twin boundary and a dissociated dislocation in <111>-oriented gold nanopillars under compression.[22] Consider an edge dislocation of Burgers vector a/2<110> dissociated into two partial dislocations of Burgers vector a/6<112> gliding on a slip plane that intersects one twin interface (Figure 3a). The reaction at the intersection between dislocation and twin boundary takes place in two stages. First, the leading partial dislocation in the incident slip is absorbed by the interface (Figure 3b). Dislocation reaction occurs, which leaves a glissile displacement shift complete (DSC) partial dislocation on the twin plane, a/6<211>, and a sessile stair-rod dislocation pinned at the twin-slip intersection, a/6<110>. The combination of the stair-rod dislocation at the intersection of stacking faults on two {111} slip planes contributes to form Lomer–Cottrell barriers. The formation of Lomer–Cottrell locks is a well-known mechanism of strengthening in bulk metals.[30–32] The atomistic results shown in Figure 3b are also in excellent agreement with the asymmetrical character of the dissociation of Lomer barriers predicted theoretically.[31]

Furthermore, when the trailing partial dislocation in turn enters the twin plane as shown in Figure 3c, a second reaction takes place where the trailing partial merges with the stair-rod dislocation obtained from the first reaction in order to form a new glissile DSC twin partial and a perfect <110> slip in the twin grain. The perfect <110> dislocation resulting from this reaction can only glide along the symmetry plane of the lock (i.e., the (001) cut plane). As a result, the twin plane is found to move upward by one atom layer along the [111] direction (Figure 3c). In this process, the initial twin boundary structure is recovered. Energetically, the first reaction corresponding to the formation of the Lomer lock, such as

$$\frac{a}{6}\left[1\bar{2}\bar{1}\right] \rightarrow \frac{a}{6}\left[2\bar{1}\bar{1}\right] + \frac{a}{6}\left[\bar{1}\bar{1}0\right] \quad ,$$

is more favorable than the second reaction given by

$$\frac{a}{6}\left[\bar{1}\bar{1}2\right] + \frac{a}{6}\left[\bar{1}\bar{1}0\right] \rightarrow \frac{a}{6}\left[11\bar{2}\right] + \frac{a}{2}\left[\bar{1}\bar{1}0\right].$$

This result implies that forming Lomer–Cottrell locks at the twin-slip intersection is made easier than transmitting the slip into a new (001) slip plane. In other words, the latter mechanism requires an increased driving force to occur. This factor could therefore play a key role in the strengthening process of twinned nanowires. Another strengthening factor could be promoted when no trailing partial dislocations are nucleated and, therefore, the second reaction does not occur. In Figure 2, this condition may be achieved when the twin interspacing is of the same size as the splitting distance for dislocation dissociation. Therefore, gaining fundamental understanding on how partial

Equations

$$\Delta E^{2D}_{trailing} \approx \frac{0.287\mu b^2\left(1-\gamma_{ssf}/2\gamma_{usf}\right)}{1-\nu/4}\left(1-\sqrt{\frac{G-\gamma_{ssf}}{(\gamma_{usf}-\gamma_{ssf})(4-3\upsilon)}}\right)^{3/2} \quad (1)$$

$$\Delta E^{2D}_{twinning} \approx \frac{0.287\mu b^2\left(1-(\gamma_{ssf}-\gamma_{stf})/2\gamma_{utf}\right)}{1-\nu}\left(1-\sqrt{\frac{G-\gamma_{ssf}}{\gamma_{utf}-\gamma_{ssf}}}\right)^{3/2} \quad (2)$$

$$\Delta E^{2D}_{nonadjacent} \approx \frac{0.287\mu b^2\left(1+\gamma_{ssf}/2\gamma_{usf}\right)}{1-\nu}\left(1-\sqrt{\frac{G-\gamma_{ssf}}{\gamma_{usf}}}\right)^{3/2} \quad (3)$$

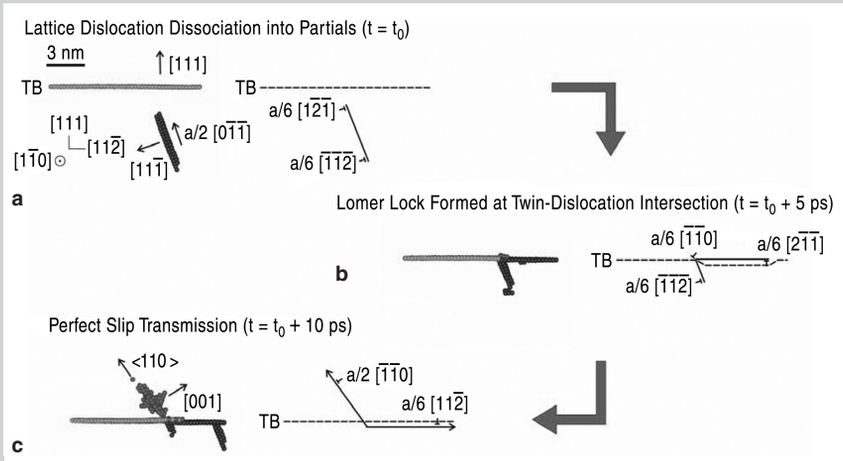

Figure 3. Multiple stages of interfacial plasticity at the intersection between a coherent Σ3 twin boundary (TB) and a dissociated lattice dislocation in a <111>-oriented gold nanopillar under compression. Slip planes and twin boundary are indicated by continuous and dashed lines, respectively. Only atoms not in perfect fcc stacking are shown. The time of simulation is indicated in parenthesis.

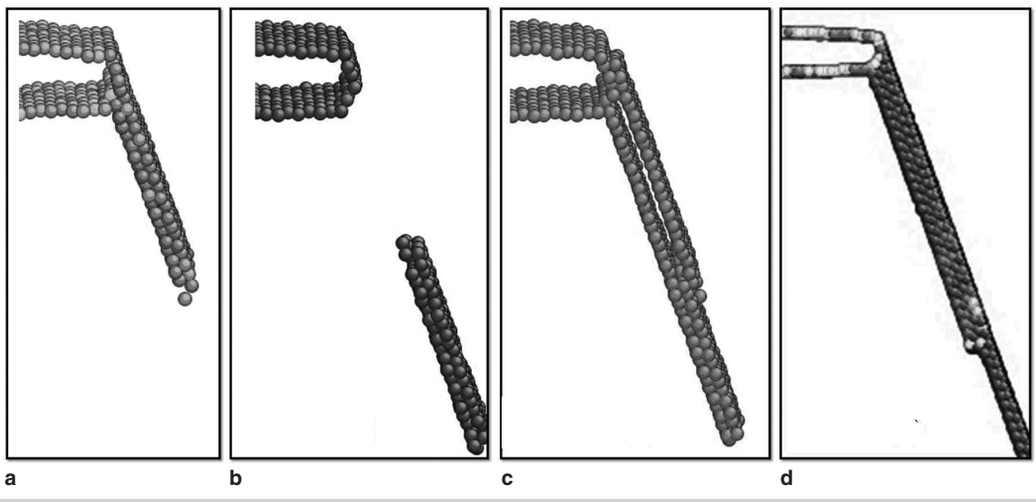

Figure 4. Images depicting partial dislocation nucleation from crack tips in fcc metals. Only atoms not in perfect fcc stacking are shown.[35] (a) Nucleation of leading partial with a stable stacking fault in its wake. (b) Nucleation of both leading and trailing partial with stable stacking fault between the two. (c) Nucleation of twinning partial after the leading partial creating a microtwin. (d) Nucleation of leading partial and a nonadjacent leading partial.

dislocations are nucleated from defects in the lattice or at free surfaces[33] is critically important to predict strengthening in twinned nanowires.

Based on the existing state of knowledge, an outlook for future research in this rich area can be summarized by asking two fundamental questions. First, can twin boundaries be an efficient means to stop the easy loss of lattice dislocations at free surfaces in metallic nanomaterials? And second, does the sample size influence the reactions occurring at twin-slip intersections? It is clearly evident from the curves presented in Figure 2 that no strengthening effects occur when the spacing between twin boundaries is larger than or equal to the diameter of the nanowire (i.e., 12 nm), because lattice dislocations are lost at free surfaces without intersecting twin boundaries. It is possible to assume here that the propensity of lattice dislocations to intersect twin boundaries would become larger as the wire diameter increases. The relationship between sample size, dislocation emission, reaction at twin boundaries, and strengthening effects, however, are not fully understood at the present.

TWIN AND PARTIAL DISLOCATION NUCLEATION

In nanowires and other nanostructured metals, Frank–Read dislocation sources are typically thought to be rare, if not completely nonexistent. Thus, dislocation nucleation from defects, free surfaces, and other stress concentrations plays a large role in the deformation of nanostructured metals. In fcc metals, the existence of partial dislocations makes several nucleation scenarios possible. While all scenarios begin with the nucleation of a "leading" partial dislocation (Figure 4a), they differ in what happens next.

The first and probably most acknowledged scenario consists of a second "trailing" partial nucleating after the first (Figure 4b). The trailing partial nucleates on the same slip plane as the leading partial and has a Burgers vector that when summed with the first gives a full dislocation. The trailing partial erases the stable stacking fault formed by the leading partial, and consequently, it enables both partials to glide as a pair freely away from the nucleation point.

A second possible scenario is that the nucleation of the leading partial is followed by the nucleation of a "twinning" partial (Figure 4c). A twinning partial is a dislocation of the same character as the leading partial and is nucleated on one of the two adjacent planes neighboring the stable stacking fault created by the leading partial. As the twinning partial propagates outward, it creates a stable stacking fault adjacent to the existing stable stacking fault. Crystallographically, this corresponds to the formation of a small twinned region of two atomic planes (i.e., a microtwin). In circumstances where nucleation is reoccurring, such as at a crack tip, additional dislocations are likely to also be twinning partials and thus will widen the twinned region.[34]

A third and rarely acknowledge scenario consists of the second partial being nucleated on a nonadjacent plane and being of the same character as the first. An example of a "nonadjacent" lagging partial is shown in Figure 4d. This scenario leads to the formation of two stable stacking faults separated by at least one plane of fcc atoms.

To predict which of the three nucleation scenarios will occur, one must know not only the interatomic potential,[36] but the loading configuration,[37] rate,[38,39] and temperature.[40] Each process must be evaluated as a thermally activated process where the average wait time at a given load for dislocation nucleation to occur is expressed as $\bar{\tau} = \nu_f^{-1} e^{\Delta E / kT}$ with ν_f being the attempt frequency, k the Boltzmann factor, T the temperature, and ΔE the activation energy. The competition between the three previously discussed nucleation cases can be condensed into a comparison of the activation energies needed for each case of lagging partial nucleation. The case with the lowest activation energy will be the one most likely to be observed.

The magnitude of the activation energy is linked to the generalized stacking fault curve.[41] Specifically, the magnitudes of its peaks and valleys, the distance between them (i.e., magnitude of the Burgers vector), and its curvature (i.e., shear modulus) all contribute. The fact that temperature influences the generalized stacking fault curve, particularly its valleys, implies that the activation energy is also a function of

temperature. The activation energy is a decreasing function of applied load and is highly dependent upon its orientation.[37, 42]

Over the past 20 years, researchers have attempted to calculate the activation energy barrier associated with dislocation nucleation through semi-analytic,[38] finite-element,[43] and atomistic analysis.[39,44] However, attaining a closed form expression clearly showing the role of each of the influencing parameters has proven challenging. Possibly the most popular and successful attempt was made by J.R. Rice and G.E. Beltz[38] in their 1992 investigation of dislocation nucleation from crack tips. They showed that in the limit of a load near that needed to drive the activation energy to zero, the activation energy associated with the nucleation of an edge dislocation leaving behind no stacking fault and coincident with a crack tip under mode II loading can be expressed as

$$\Delta E^{2D} \approx \frac{0.287\mu b^2}{1-\nu}\left(1-\sqrt{G/G_{crit}}\right)^{3/2}$$

where μ, ν, and b are the shear modulus, Poisson's ratio, and Burgers vector, respectively. G represents the strain energy release rate of the applied loading, and G_{crit} the strain energy release rate at which the activation energy goes to zero.

To approximate ΔE^{2D}, for the nucleation of the lagging partials from the simplified geometry specified above, Rice and Beltz's expression must be altered to include several additional features. First, the influence of the leading partial on the stress field at the crack tip must be incorporated. Second, the role of the lagging partial must be included in that it either erases stacking fault and creates two twinning faults, or solely creates stacking fault. Finally, for the trailing partial case, a difference in Burgers vector orientation must also be included. Thus, for the limiting case of geometry and loading orientation, where trailing partial dislocation nucleation is the most difficult, approximations for the two-dimensional (2-D) activation energy of each of the scenarios are presented in the equations table.

Central to the approximations is the relationship for crack tip shielding and fault annihilation and/or creation. For crack tip shielding

$$K_{II}^{Shielded} = K_{II} - \frac{\mu b_p}{(1-\nu)\sqrt{2\pi r}}$$

is used, where K_{II} is the mode II stress intensity factor and r is the distance that the leading partial is away from the crack tip.[36] For fault annihilation and/or creation we multiply by a term

$$\left(1 - \frac{\gamma_1 - \gamma_3}{2\gamma_2}\right) \text{ where } \gamma_1, \gamma_2, \text{ and } \gamma_3$$

represent the fault energies corresponding to displacements of 0, $b_p/2$, and b_p on the plane over which the lagging partial nucleates.[39]

In Equations 1–3 there is a minimum load or strain energy release rate, $G = \gamma_{ssf}$, below which thermally activated nucleation of the second partial dislocation will not occur. The minimum energy release rate, G_{min}, arises from the requirement that the applied load be sufficient to sustain the equilibrium existence of the leading partial dislocation ahead of the crack tip. Since the term inside the 3/2 power goes to zero in Equations 1–3 when $G = G_{min}$, a comparison of the 2-D maximum energy barriers is straightforward. Assuming that $\gamma_{stf} \approx \gamma_{ssf}$, $\Delta E_{nonadjacent} > \Delta E_{twinning} > \Delta E_{trailing}$ at $G = G_{min}$, making trailing partial nucleation favorable at this limiting load.

From Equations 1–3 the energy release rates at which the energy barriers go to zero are given as γ_{utf}, $\gamma_{usf} + \gamma_{ssf}$, and $\sim (3\gamma_{usf} - 2\gamma_{ssf})$ for the twinning, nonadjacent, and trailing partial cases, respectively. Taking the room-temperature stacking fault values of various fcc metals from the literature[37,39] suggests that for Al, Ag, Au, Cu, Ir, Ni, and Pt, twinning is favorable at high loads and/or loading rates while trailing partial emission becomes favorable at lower loads and/or loading rates. From Equations 1–3 and the values of the fcc stacking fault energies in the literature[37,39] it appears that nonadjacent partial emission is associated with a higher 2-D energy barrier than twin emission over the entire range of admissible loads. Nonetheless, it is important to recognize that the difference in energy barriers between twinning and nonadjacent partial emission can be small, such as for silver. It is very possible that nonadjacent partial emission would occur at crack tips in some materials, especially considering the uncertainty surrounding the values of unstable stacking fault energies.[37]

In summary, Equations 1–3 are intended to give insight into the factors controlling the competition between full dislocation nucleation, twin nucleation, and non-adjacent leading partial nucleation. Even though they represent only 2-D estimations, they give insight into the differences observed across materials and effects arising out of the limited thermal activation available in atomistic simulations. Moreover, understanding how dislocation nucleation unfolds in nanostructured metals sheds light on not only their yield strength but also their ductility, reliability, and, ultimately, their performance.

CONCLUSIONS

This overview has clearly shown that the role of twin boundaries is ubiquitous for both synthesis and properties in nano-enhanced fcc metals. Meaningful results related to strength and plasticity of twinned nanomaterials, however, can only be achieved if the influences of microstructure and sample size are fully understood. A suggested approach is to take full advantage of combining experimental methods with innovative atomistic simulations. By way of analogy, early results from this combination of methodologies have been very successful in the mechanical characterization of solid metal surfaces and thin films. An outcome is the strong potential for novel plasticity mechanisms to be discovered at limited length scale that will enhance size-dependent properties in fcc metals.

ACKNOWLEDGEMENTS

Frederic Sansoz gratefully acknowledges support from the National Science Foundation (NSF) CAREER program (grant no. DMR-0747658). Hanchen Huang would like to thank the NSF for support (grants no. CMMI-0553300 and CMMI-0727413). Derek Warner acknowledges support from the Office of Naval Research, Ship Systems and Engineering Division (N000014-08-0862).

References

1. J. Wang (Ph.D. thesis, Rensselaer Polytechnic Institute, 2006).
2. Y. Mishin et al., *Phys. Rev. B,* 63 (2001), no. 224106.

3. J. Wang, H. Huang, and T.S. Cale, *Modelling Simul. Mater. Sci. Eng.,* 12 (2004), pp. 1209–1225.
4. S. Ino, *J. Phys. Soc. Jpn.*, 21 (1966), p. 346.
5. A.S. Barnard, *J. Phys. Chem. C*, 112 (5) (2008), pp. 1385–1390.
6. J. Wang and H. Huang, *MRS Proceedings,* 849 (2004), pp. 91–96.
7. H. Huang et al., *Appl. Phys. Lett.,* 81 (2002), pp. 4359–4361.
8. H.W. Shim and H. Huang, *Appl. Phys. Lett.*, 90 (2007), p. 83106-1-3.
9. H.W. Shim and H. Huang, *Nanotechnology,* 18 (2007), p. 335607-1-5.
10. J. Wang et al., *Nano Lett.*, 5 (2005), pp. 2505–2508.
11. S.J. Liu, H. Huang, and C.H. Woo, *Appl. Phys. Lett.,* 80 (2002), pp. 3295–3297.
12. S.K. Xiang and H. Huang, *Appl. Phys. Lett., 92* (2008), no. 101923.
13. L.G. Zhou and H. Huang, *Phys. Rev. Lett.* (2008), under revision.
14. X. Zhang et al., in this issue.
15. V. Yamakov et al., *Acta Mater.*, 51 (2003), pp. 4135–4147.
16. X. Zhang et al., *Appl. Phys. Lett.*, 84 (7) (2004), pp. 1096–1098.
17. J. Diao, K. Gall, and M.L. Dunn, *Nano Lett.*, 4 (2004), p. 1863.
18. B. Hyde, H.D. Espinosa, and D. Farkas, *JOM*, 57 (9) (2005), p. 62.
19. Z.H. Jin et al., *Scr. Mater.*, 54 (2006), p. 1163.
20. J. Wang and H. Huang, *Appl. Phys. Lett.,* 88 (2006), no. 203112.
21. T. Zhu et al., *Proc. Natl. Acad. Sci. U.S.A.*, 104 (2007), p. 3031.
22. K.A. Afanasyev and F. Sansoz, *Nano Lett.,* 7 (7) (2007), pp. 2056–2062.
23. Z. Chen, Z. Jin, and H. Gao, *Phys. Rev. B,* 75 (2007), no. 212104.
24. M.P. Dewald and W.A. Curtin, *Phil. Mag.,* 87 (2007), pp. 4615–4641.
25. Z.-H. Jin et al., *Acta Mater.,* 56 (2008), pp. 1126–1135.
26. B. Wu, A. Heidelberg, and J.J. Boland, *Nature Materials,* 4 (2005), p. 525.
27. B. Wu et al., *Nano Lett.*, 6 (3) (2006), pp. 468–472.
28. A.J. Cao and Y.G. Wei, *Phys. Rev. B*, 74 (2006), no. 214108.
29. A.J. Cao, Y.G. Wei, and S.X. Mao, *Appl. Phys. Lett.,* 90 (2007), no. 151919.
30. J.P. Hirth and J. Lothe, *Theory of Dislocations* (New York: McGraw-Hill, 1968).
31. J. Bonneville and J. Douin, *Phil. Mag. Lett.*, 62 (1990), p. 247.
32. M.I. Baskes, R.G. Hoagland, and T. Tsuji, *Modelling Simul. Mater. Sci. Eng.*, 6 (1998), p. 9.
33. H.S. Park, K. Gall, and J.A. Zimmerman, *J. Mech. Phys. Solids,* 54 (9) (2006), pp. 1862–1881.
34. D. Farkas et al., *Phil. Mag. A,* 81 (5) (2001), pp. 1241–1255.
35. J. Li, *Modelling Simul. Mater. Sci. Eng.*, 11 (2) (2003), pp. 173–177.
36. J.R. Rice, *J. Mech. Phys. Solids,* 40 (2) (1992), pp. 239–271.
37. E.B. Tadmor and N. Bernstein, *J. Mech. Phys. Solids,* 52 (11) (2004), pp. 2507–2519.
38. J.R. Rice and G.E. Beltz, *J. Mech. Phys. Solids,* 42 (2) (1994), pp. 333–360.
39. D.H. Warner, W.A. Curtin, and S. Qu, *Nature Materials*, 6 (11) (2007), pp. 876–881.
40. R. Meyer and L.J. Lewis, *Phys. Rev. B*, 66 (5) (2002), no. 052106.
41. H. Van Swygenhoven, P.M. Derlet, and A.G. Froseth, *Nature Materials,* 3 (6) (2004), pp. 399–403.
42. E.B. Tadmor and S. Hai, *J. Mech. Phys. Solids,* 51 (5) (2003), pp. 765–793.
43. G. Xu, A.S. Argon, and M. Ortiz, *Phil. Mag. A,* 75 (2) (1997), pp. 341–367.
44. T. Zhu et al., *Phys. Rev. Lett.,* 100 (2) (2008), no. 025502.

Frederic Sansoz is with the School of Engineering and Materials Science Program, University of Vermont, Burlington, Vermont; Hanchen Huang is with the Department of Mechanical, Aerospace and Nuclear Engineering, Rensselaer Polytechnic Institute, Troy, New York; and Derek H. Warner is with the School of Civil and Environmental Engineering, Cornell University, Ithaca, New York. Prof. Sansoz can be reached at (802) 656-3837; fax (802) 656-1929; e-mail frederic.sansoz@uvm.edu.